# A model-based projection of historical state of a coastal ecosystem: relevance of phytoplankton stoichiometry

Onur Kerimoglu[a,*], Fabian Große[b,1], Markus Kreus[c,2], Hermann-J. Lenhart[b], Justus E.E. van Beusekom[a]

[a]*Institute for Coastal Research, Helmholtz Zentrum Geesthacht, Geesthacht, Germany*
[b]*Department of Informatics, University of Hamburg, Hamburg, Germany*
[c]*Institute of Oceanography, University of Hamburg, Hamburg, Germany*

## Abstract

We employed a coupled physical-biogeochemical modelling framework for the reconstruction of the historic ($H$), pre-industrial state of a coastal system, the German Bight (southeastern North Sea), and we investigated its differences with the recent, control ($C$) state of the system. According to our findings: i) average winter concentrations of dissolved inorganic nitrogen and phosphorus (DIN and DIP) concentrations at the surface are ∼70-90% and ∼50-70% lower in the $H$ state than in the $C$ state within the nearshore waters, and differences gradually diminish towards off-shore waters; ii) differences in average growing season chlorophyll $a$ (Chl) concentrations at the surface between the two states are mostly less than 50%; iii) in the off-shore areas, Chl concentrations in the deeper layers are affected less than in the surface layers; iv) reductions in phytoplankton carbon (C) biomass under the $H$ state are weaker than those in Chl, due to the generally lower Chl:C ratios; v) in some areas the differences in growth rates between the two states are negligible, due to the compensation by lower light limitation under the $H$ state, which in turn explains the lower Chl:C ratios; vi) zooplankton biomass, and hence the grazing pressure on phytoplankton is lower under the $H$ state. This trophic decoupling is caused by the low nutritional quality (i.e., low N:C and P:C) of phytoplankton. These results call for increased attention to the relevance of the acclimation capacity and stoichiometric flexibility of phytoplankton for the prediction of their response to environmental change.

*Keywords:* eutrophication, pristine conditions, reconstruction, adaptation, acclimation

## 1. Introduction

Trophic states of many coastal systems throughout the world have been, and are being rapidly altered due to anthropogenic activities (e.g. Artioli et al., 2008; Diaz & Rosenberg, 2008; Smith & Schindler, 2009; Cai et al., 2011). In Europe, industrialization and population growth resulted in intense eutrophication of coastal systems until the 1980s, followed by oligotrophication, owed to mitigation measures (Artioli et al.,

---
[*]orresponding author
*Email address:* kerimoglu@gmail.com (Onur Kerimoglu)
[1]Present address: Department of Oceanography, Dalhousie University, Halifax, NS, Canada
[2]Present address: Federal Waterways Engineering and Research Institute, Hamburg, Germany

2008). In the 1980s, the North Sea was one of those severely eutrophied coastal systems, due to the emissions of several densely populated and industrialized countries (Emeis et al., 2015).

The German Bight, located at the southeastern edge of the North Sea (Fig. 1) is particularly prone to be impacted by eutrophication, because of the major fluxes by the Elbe River (Pätsch et al., 2010), the along-shore cyclonic currents bringing the nutrient-enriched coastal waters (Pätsch et al., 2010; Callies & Scharfe, 2015), trapping of the nutrients in the Regions of Freshwater Influence (ROFI) and the estuarine-like circulation (Burchard et al., 2008; Flöser et al., 2011). Within the 20th century, there have been drastic changes in the nutrient loading rates to the system. For instance, historic observations from the Rhine River show that nitrogen (N) and phosphorus (P) concentrations remained at a low level until the 1940s (van Bennekom & Wetsteijn, 1990), sharply increased since the 1970s and reached a maximum during the 1980s (van Beusekom & de Jonge, 2002). Especially P, but also N loading rates by other major continental rivers discharging to the system have been decreasing since the 1990s (Radach & Pätsch, 2007; Claussen et al., 2009). In response to these reduction in riverine loadings, coastal areas of the German Bight have been in an oligotrophication trend (Claussen et al., 2009; Wiltshire et al., 2010; van Beusekom et al., 2017).

Assessing the eutrophication status of an ecosystem is not a straightforward task. For the North Sea, the 'Common Procedure' of the Oslo and Paris (OSPAR) commissions defines a set of ecological quality objectives and indicators, which refer to the 'historical background levels' (OSPAR, 2013). The concept of background concentrations was used for the assessment of estuaries in the USA as well (Bricker et al., 2003). Similarly, the European Commission's Water Framework Directive (WFD), which is concerned with improving the ecological status of the surface waters in Europe, including the transitional, coastal and marine waters, requires definition of their 'reference conditions' (EC, 2000, 2009). The hierarchical preference of approaches for defining the reference conditions are specified by the WFD to be: 1) referring to existing undisturbed, or minimally disturbed sites; 2) using historical data and information; 3) models; and 4) expert judgement (CIS-COAST, 2003). Deriving the reference conditions based on the available observation data is recognized to be difficult (EC, 2009), as often such minimally disturbed sites are non-existent, and available monitoring data do not cover the undisturbed conditions. Given these difficulties, a number of modelling approaches has been used for estimating the reference conditions of systems like the North Sea and the Baltic Sea (e.g., Schernewski & Neumann, 2005; Topcu et al., 2011; Lancelot et al., 2014; Desmit et al., 2018).

For the North Sea and the German Bight in specific, a particular statistical modelling approach has been to extrapolate the available data on historical riverine nutrient concentrations seawards, based on the relationships between nutrient concentrations and salinities, and assuming conservative mixing (e.g., van Raaphorst et al., 2000; van Beusekom, 2005; Laane et al., 2005; Brockmann et al., 2007; Topcu et al., 2011). Similarly, the present-day relationships between the nutrient concentrations and chlorophyll $a$ (Chl) concentrations (e.g., Nielsen et al., 2002; van Beusekom, 2005; Smith, 2006) were used to estimate the background values of the latter (e.g., van Beusekom, 2005; Laane et al., 2005; Brockmann et al., 2007; Topcu et al., 2011; van Beusekom et al., 2017). These statistical approaches are subject to shortcomings, such as the inaccuracy

of the conservative mixing assumption (van Raaphorst et al., 2000), the present-day empirical relationships possibly being invalid under different environmental conditions (Duarte et al., 2009), and the caveats of using the cross-system relationships (e.g. as in Smith, 2006) for estimating the response of a given system.

⁴⁵ As an alternative approach, coupled physical-biogeochemical models have been used for the reconstruction of pristine conditions of the Baltic Sea (Schernewski & Neumann, 2005) and the North Sea (Lancelot et al., 2014; Desmit et al., 2015). In a wider context of the eutrophication problem, such models have been successfully applied to a number of systems, including, but not limited to; the North Sea (Lenhart et al., 2010), the Baltic Sea (Neumann et al., 2002), the Black Sea (Salihoglu et al., 2017), the Mediterrenean Sea (Macias & ⁵⁰ Stips, 2017) and the Gulf of Mexico (Laurent et al., 2012). Coupled physical-biogeochemical models do not only provide insight into how the ecosystems may behave under different environmental forcing, but they also serve in gaining understanding of the specific mechanisms responsible for the observed and predicted phenomena.

In this study, we use such a coupled physical-biogeochemical modelling framework to construct the his- ⁵⁵ torical conditions of the German Bight. We first construct the nutrient loading conditions for the 1880 conditions, using realistic nutrient riverine and atmospheric flux estimates. We employ these historical nutrient loading conditions to force a 3-D coupled model system of the southern North Sea (SNS) to construct the historic state of the system. We then perform an in-depth analysis of the differences between the recent and historic states of the German Bight. We focus particularly on phytoplankton and the relevance of the ⁶⁰ adaptive changes in their physiological state, as an aspect that has been often ignored in previous studies.
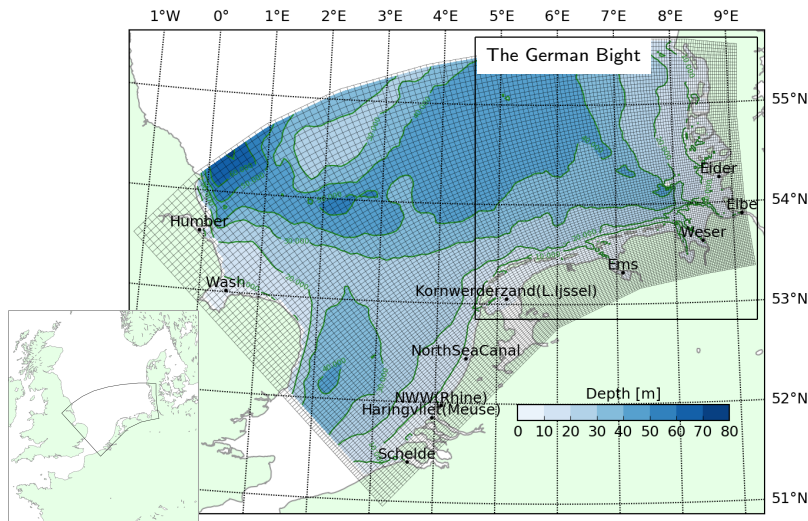


Figure 1: Position and bathymetry of the model domain, location of rivers considered in this study and the German Bight. Gray lines display the model grid.

## 2. Materials and Methods

### 2.1. The Modelling Framework

For the construction of the recent (or control; $C$) and historic ($H$) states of the SNS, we used the coupled physical-biogeochemical model system recently introduced by Kerimoglu et al. (2017). Dynamics of the pelagic biogeochemistry is described by the Model for Adaptive Ecosystems in Coastal Seas (MAECS), which, otherwise similar to other ecosystem models with respect to the recycling of the organic and inorganic macro-nutrients (carbon (C), N and P), includes an optimality based physiological acclimation model of phytoplankton growth (Wirtz & Kerimoglu, 2016). MAECS is further coupled to a simple, 2-D benthic diagenesis model in order to account for the benthic-pelagic exchange. The full model description, and an extensive model performance assessment for the period 2000-2010 (same period employed in the current study) is provided by Kerimoglu et al. (2017). Some aspects of the model directly relevant for the current study are described in detail below.

#### 2.1.1. Acclimation of phytoplankton

As the most relevant aspect of the acclimation scheme (Wirtz & Kerimoglu, 2016) to the current study, fractional allocations to the light harvesting, carboxylation and nutrient acquisition machineries are resolved by the physiological trait variables ($f_{LH}$, $f_C$ and $f_V$ respectively). The former two are represented by state variables, and the $f_V$ is given as the remaining fraction of the total allocation pool ($f_V = 1 - f_{LH} - f_C$). Dynamics of the dynamic allocation traits, $f$ ($= f_{LH}$, $f_C$), are given by:

$$\frac{\mathrm{d}}{\mathrm{d}t}f = \delta_f \cdot \left[ \frac{\partial V_C}{\partial f} + \sum_X \frac{\partial V_C}{\partial Q_X} \frac{\partial Q_X}{\partial f} \right] \tag{1}$$

where $\delta_f$ is the trait flexibility, X expands to nutrients (N,P), $Q_X$ is the molar ratio of the nutrients to C bound to phytoplankton, and $V_C$ is the C uptake rate. The trait flexibility term $\delta_f$ is heuristically set to $\delta_f = f \cdot (1-f)$ to maintain stability.

It is worth noting also that the $f_{LH}$ is proportional to the Chl concentration in chloroplasts ($\theta$), hence the Chl:C ratio of phytoplankton:

$$\theta = \theta_C \cdot \frac{f_{LH}}{q_N f_C} \tag{2}$$

where $\theta_C$ is a proportionality coefficient and $q_N$ is the relative, normalized N quota of phytoplankton. Wirtz & Kerimoglu (2016) provide the full details of the dynamic acclimation scheme.

#### 2.1.2. Resource limitation of phytoplankton

Growth allowance of phytoplankton by light is estimated by

$$A_L = f_C \cdot \left( 1 - e^{-\alpha \theta \mathrm{PAR}/P_{\max}} \right) \tag{3}$$

4

where, $\alpha$ is the light absorption coefficient, PAR is the photosynthetically available radiation, $P_{\text{max}}$ is the maximum photosynthesis rate. Growth allowance by N and P is estimated by the relative quota (X:C ratio) of the cells , given by:

$$A_X = \frac{Q_{\text{X}} - Q_{\text{X}}^0}{Q_{\text{X}}^* - Q_{\text{X}}^0} \tag{4}$$

where $Q_{\text{X}}^0$ is the subsistence quota and $Q_{\text{X}}^*$ is the reference quota.

In order to avoid confounding effects of extreme values within the surface and bottom layers (e.g., too low nutrient and light allowances, respectively), which may not be necessarily relevant because of possibly very small phytoplankton concentrations, all these quantities ($A_L$, $A_N$, $A_P$), and the resulting specific growth rate of phytoplankton are presented in terms of biomass-weighted vertical averages.

## 2.1.3. Influence of phytoplankton stoichiometry on zooplankton

Zooplankton, which feed on phytoplankton with variable stoichimetry, are assumed to maintain their stoichiometric homestasis (Sterner & Elser, 2002) through adjustment of their excretion ($M_{ex}$) and egestion ($M_{eg}$) rates of C, N and P. The Potential excretion rate of N, $M'_{ex,\text{N}}$, is given by the sum of a background excretion rate, and an adjustment term that results from the excess or lack of N in the ingested food:

$$M'_{ex,\text{N}} = m_{ex} \cdot Z_{\text{N}} + \gamma \cdot G_{\text{C}} \cdot (P_{\text{N:C}} - Z_{\text{N:C}}) \tag{5}$$

where $m_{ex}$ is a rate constant, $Z_{\text{N}}$ is N bound to zooplankton, $\gamma$ is assimilation efficiency, $G_C$ is grazing rate in terms of C, and $P_{\text{N:C}}$ and $Z_{\text{N:C}}$ are the N:C ratio of phytoplankton and zooplankton, respectively. For $P_{\text{N:C}} \ll Z_{\text{N:C}}$, the negative stoichiometric adjustment term may exceed the background excretion rate, resulting in $M'_{ex,\text{N}} < 0$. Such a biologically implausible operation is avoided using a threshold function for the effective excretion rate ($M_{ex,\text{N}} = \max(0, M'_{ex,\text{N}})$), and using $M'_{ex,\text{N}}$ to adjust (reduce) the potential egestion rate of N:

$$M'_{eg,\text{N}} = \begin{cases} (1-\gamma) \cdot G_{\text{C}} \cdot Z_{\text{N:C}}, & \text{if } M'_{ex,\text{N}} \geq 0 \\ (1-\gamma) \cdot G_{\text{C}} \cdot Z_{\text{N:C}} + M'_{ex,\text{N}}, & \text{otherwise} \end{cases} \tag{6}$$

The (negative) adjustment term ($M'_{ex,\text{N}}$) may exceed the base egestion rate ($(1-\gamma) \cdot G_C \cdot Z_{N:C}$), resulting in $M'_{eg,\text{N}} < 0$. This biologically implausible operation is again avoided using a threshold function ($M_{eg,\text{N}} = \max(0, M'_{eg,\text{N}})$), and the negative $M'_{eg,\text{N}}$ is interpreted as the relative N-shortage, equivalently C-surplus, which is therefore used to adjust (increase) the C excretion rate:

$$M_{ex,\text{C}} = \begin{cases} m_{ex} \cdot Z_C, & \text{if } M'_{eg,\text{N}} \geq 0 \\ m_{ex} \cdot Z_C - M'_{eg,\text{N}} \cdot Z_{\text{C:N}}, & \text{otherwise} \end{cases} \tag{7}$$

Exretion/egestion adjustment of P, and the corresponding readjustment of C excretion are identical to those given for N (Eqs. 5-7). At the final step, to satisfy the N:P balance, the potentially negative $M'_{eg,\text{P}}$

<sub>120</sub> caused by the P-shortage is used to readjust the excretion rate of N, analogous to the readjustment of the C excretion (Eq. 7):

$$M_{ex,\mathrm{N}} = M_{ex,\mathrm{N}} - M'_{eg,\mathrm{P}} \cdot Z_{\mathrm{N:P}}, \quad \text{if } M'_{eg,\mathrm{P}} \leq 0 \tag{8}$$

Further information on zooplankton dynamics, including growth and losses to higher trophic levels can be found in (Kerimoglu et al., 2017).

<sub>125</sub> *2.1.4. Model coupling and boundary nutrient fluxes*

MAECS was coupled to the General Estuarine Transport Model (GETM; Burchard & Bolding, 2002) as the hydrodynamical host, through the Framework for Aquatic Biogeochemical Models (FABM; Bruggeman & Bolding, 2014). We used 20 terrain-following layers and a curvilinear grid, resolution of which varies between 1.5-4 km (Fig. 1). The model system was forced with realistic meteorological conditions, riverine fluxes by <sub>130</sub> 11 major rivers (9 continental, 2 in the UK; see Fig. 1) and atmospheric deposition (Kerimoglu et al., 2017). At the open ocean boundaries, phytoplankton and zooplankton were assumed to be at zero gradient, whereas all other biogeochemical variables were nudged to the values estimated by the ECOsystem Model HAMburg (ECOHAM; Lorkowski et al., 2012; Große et al., 2016), which was forced with the riverine and atmospheric N deposition fluxes consistent with the eutrophication state under consideration.

<sub>135</sub> *2.2. Construction of the control and historic states*

We considered two states of the system: the control ($C$) and historic ($H$). The $C$ state refers to the recent conditions for the period 2000-2010, while the historic state corresponds to the pre-industrial state of the system as of 1880 regarding the nutrient fluxes to the system (Schöpp et al., 2003; Hirt et al., 2014). In order to make the model results independent from an arbitrary set of prescribed initial conditions, the model was <sub>140</sub> spun up 4 times for the first simulation year for each state. Annual cycles of all pelagic and benthic variables in the 3rd spin-up year have been observed to be almost identical to those in the 4th repetition, which was included in the analyses presented here. Detailed information on the reconstruction of these two states are provided below.

*2.2.1. C: Control state*

<sub>145</sub> For the $C$ state corresponding to the period 2000-2010, we used measured N and P fluxes from nine major continental rivers (Pätsch et al., 2016) and two major british rivers (van Leeuwen, pers. comm.), and atmospheric N deposition rates estimated by EMEP (European Monitoring and Evaluation Programme, http://www.emep.int). The $C$ state, especially within the German Bight, compares well with a wide array of observations (Kerimoglu et al., 2017), and thus can be considered to be a realistic representation of the <sub>150</sub> recent state of the system.

*2.2.2. H: Historic state*

We refer to the conditions around 1880 as the $H$ state of the system, as this was the earliest date with reliable data for estimating the external nutrient inputs (e.g., Schöpp et al., 2003; Hirt et al., 2014). The construction of the riverine nutrient loads in the $H$ state were based on the estimates of the river basin model 'Modelling of Nutrient Emissions in River Systems' (MONERIS Venohr et al., 2011), for the total N (TN), Dissolved Inorganic N (DIN), and total P (TP) concentrations at the limnic-marine boundaries of the major continental rivers for the year 1880 (Gadegast & Venohr, 2015). For estimating the nutrient concentrations in 1880, MONERIS was forced with input data constructed with the available information on the land use, distribution of crops, live stock, population, connectedness to sewer systems and atmospheric deposition within the drainage basin (Gadegast & Venohr, 2015; Hirt et al., 2014). Moreover, parameters concerning the P concentrations in groundwater and soil, per capita emissions and water usage, emissions from streets by animals and litter, and TN and TP retention in treatment plants were adjusted to the 1880 conditions (Table 6 in Gadegast & Venohr, 2015; Hirt et al., 2014). The extensive manipulation of the historical marshlands and floodplains of major rivers such as the Elbe and Rhine is considered to have eliminated the denitrification potential at the outlets of these rivers (de Jonge & de Jong, 2002; Dähnke et al., 2008; Deek et al., 2013), whereas MONERIS does not consider such hydromorphological changes (Hirt et al., 2014). To account for this fact, and given that as much as 40% of the N in the Elbe estuary was estimated to be removed by denitrification in the 1980s (Schröder et al., 1996), and the upper bound for N removal in estuaries is about 50% (Seitzinger, 1988), we assume the N concentrations at the river mouths to be 50% lower than the estimates of MONERIS for the $H$ state. An overview of the nutrient concentrations for the rivers used in the $H$ scenario is given in Table 1.

Table 1: Nutrient concentrations (mg/L) at the river mouths under the historic ($H$) state.

| River name | TN | DIN | TP |
|---|---|---|---|
| Rhine | 0.705 | 0.570 | 0.03 |
| Meuse | 1.250 | 1.065 | 0.05 |
| Lake Ijssel | 0.740 | 0.370 | 0.04 |
| Ems | 0.925 | 0.725 | 0.03 |
| Weser | 0.895 | 0.745 | 0.03 |
| Elbe | 0.975 | 0.730 | 0.05 |
| Eider | 0.710 | 0.560 | 0.02 |

For calculating the daily riverine nutrient loading rates in the $H$ state for each river, we calculated percentage reduction factors, $R$, required to reduce the discharge-weighted average concentration over the period 2000-2010 to the historical concentration estimates listed in Table 1, according to:

$$R = 100 \cdot \left( 1 - \frac{\mathrm{X}_H}{\sum(Q \cdot \mathrm{X}_C)/\sum Q} \right) \tag{9}$$

where $\mathrm{X}_H$ and $\mathrm{X}_C$ (X=TN, DIN, TP) are the average historic concentration (Table 1) and daily measured

concentration for the period 2000-2010, respectively, and $Q$ is the daily measured freshwater discharge. For DIN and organic N (ON), individual reduction percentages were calculated using the historical concentrations for TN and DIN, and assuming that the difference is the ON (Table 2). The reduction percentage found for TP was assumed to hold equally for both DIP and OP (Table 2). For the rivers not included in Table 1, the reduction percentages were assumed to be equal to the discharge-weighted average reduction values.

Table 2: Percentage (%) reduction factors based on the discharge-weighted average nutrient concentrations during the period 2000-2010 for obtaining the riverine loadings under the historic (1880) conditions (Eq. 9). For the rivers for which the historic concentrations were not available, discharge-weighted average reduction factors (*) were used.

| River name | DIN | ON | DIP & OP |
|---|---|---|---|
| Rhine | 79 | 72 | 81 |
| Meuse | 66 | 65 | 66 |
| Lake Ijssel | 78 | 70 | 67 |
| Ems | 86 | 80 | 82 |
| Weser | 81 | 80 | 83 |
| Elbe | 80 | 60 | 73 |
| Eider | 78 | 89 | 90 |
| Schelde | * | * | * |
| Nordzeekanaal | * | * | * |
| Seine | * | * | * |
| other French rivers | * | * | * |
| UK rivers | * | * | * |
| average (*) | 77 | 69 | 75 |

For the atmospheric N deposition rates, EMEP estimates were extrapolated back to 1880 based on scaling factors extracted from Schöpp et al. (2003), following the procedure described in Große et al. (2016). Total ($NO_x$+$NH_3$) N deposition rates estimated for 1880 based on this approach correspond to 30.8% of the EMEP estimates averaged over 2000-2010.

## 3. Results

### 3.1. Nutrient Fluxes

The riverine and atmospheric deposition fluxes resulting from the assumptions and calculations above (Section 2.2), employed for the $C$ and $H$ states of the system are provided in Figs. 2 and 3, respectively. For the continental rivers, the TN and TP loading rates are largely proportional with the discharge rates, while for especially the TP loading by Humber is disproportionately high, indicating relatively higher concentrations in this river. Atmospheric N deposition rates are about 2-3 fold higher in the near-shore regions than in the off-shore regions under the $C$ state, which, by definition, applies to the $H$ state as well.

### 3.2. Simulated Chlorophyll, DIN and DIP

Climatological growing season (April–September) average Chl and winter (December–February) average DIN and DIP concentrations at the surface layer estimated for the $C$ and $H$ states and relative percentage
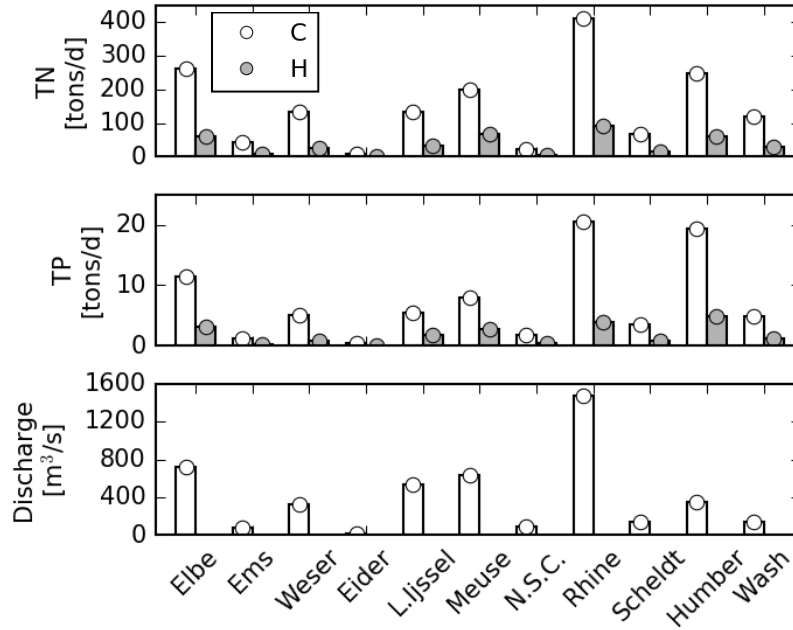
Figure 2: 2000-2010 daily average TN and TP loads and discharge rates for each river used as model forcing for control ($C$) and historic ($H$) states (discharge rates are assumed to be identical for both states). N.S.C: North Sea Channel.
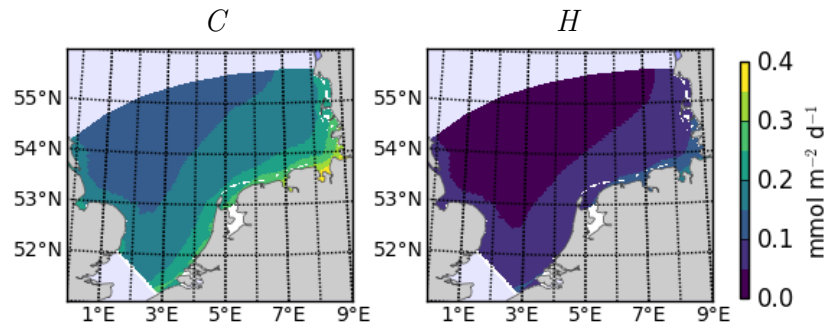


Figure 3: 2000-2010 average daily N deposition rates used as model forcing for $C$ and $H$ states. The color scale applies to both panels.

differences are provided in Fig. 4. The differences in nutrient concentrations are most pronounced within the near-shore regions, reaching down to 70-90% for DIN and to 50-70% for DIP. The differences in Chl do not show the regular cross-shore gradients displayed by the nutrients, and are in general weaker than those in the nutrients. Historical values are mostly 10-30% lower than the control values, more than 30% lower only within the western and northern margins of the Wadden Sea and within a large off-shore patch, and not considerably different ($\pm 10\%$) or even slightly higher (up to $\sim 20\%$) close to the Elbe mouth.

The Chl, DIN and DIP concentrations estimated by the $C$ and $H$ model runs and measured at the five monitoring stations, Norderelbe, Helgoland, T11, Norderney and Sylt are shown in Fig. 5a-e, respectively. The former three form a transect (Fig. 5f), along which the differences between the $C$ and $H$ states in
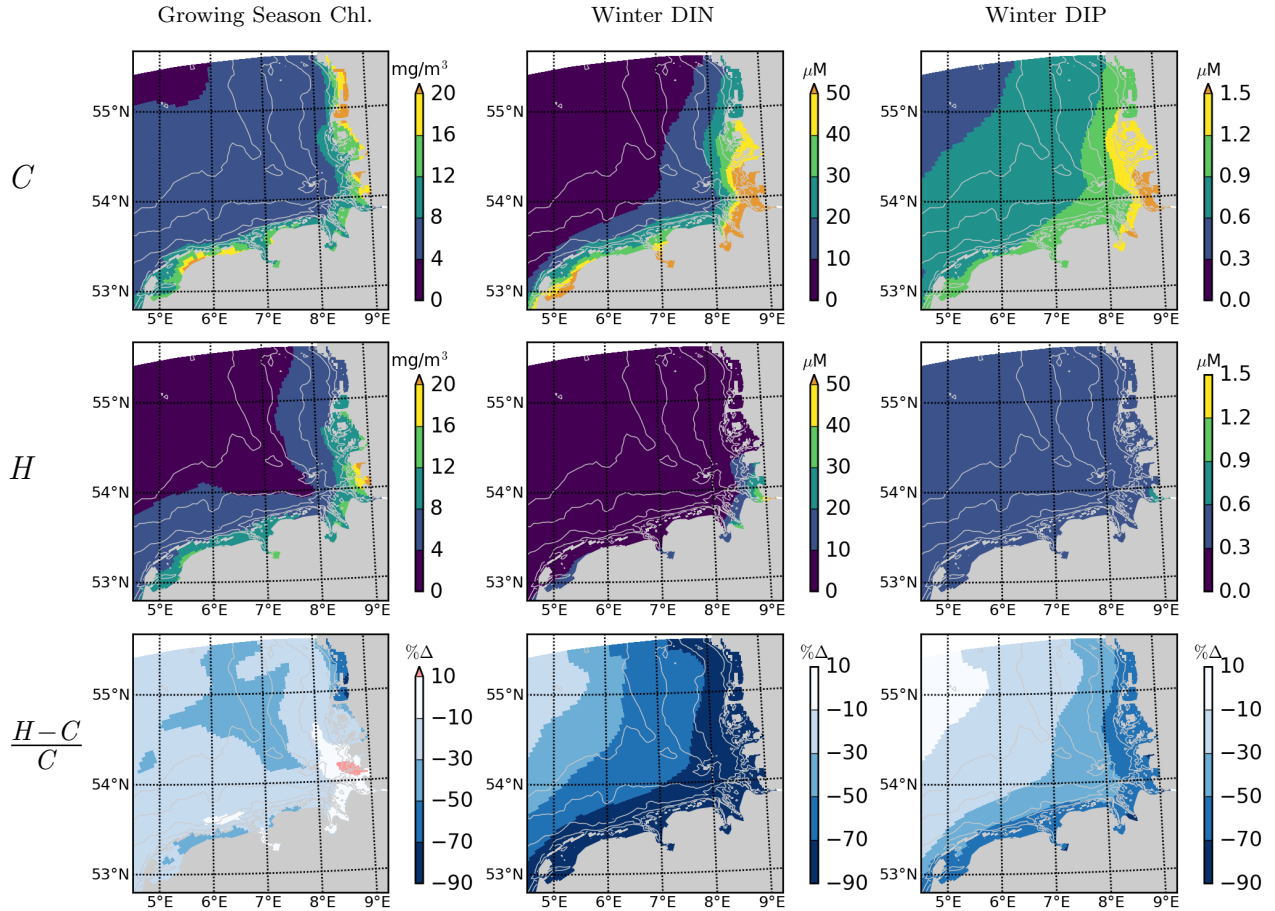
9

Figure 4: 2000-2010 growing season (March-September) climatological average Chl and winter (Dec-Feb) average DIN, DIP concentrations at the surface layer according to the control ($C$) and historic ($H$) states, and the relative percentage differences.

nutrients and surface Chl form opposite gradients; those in Chl being smallest and nutrients being largest at the mouth of the Elbe river (as represented by the station Norderelbe; Fig. 5a), and vice versa at the off-shore end of the transect (as represented by the station T11, Fig. 5c). At the Norderelbe, and the two coastal stations, Norderney and Sylt, especially DIN, but also DIP concentrations are considerably lower in the $H$ state than in the $C$ state. At the two off-shore stations, Helgoland and T11, the reductions in DIN are also considerable, whereas the differences in DIP are subtle. At all stations, the early spring Chl concentrations estimated for the $H$ state are higher. At the Norderelbe station, Chl during the spring bloom reaches slightly higher concentrations under the $H$ state relative to the $C$ state. At all other stations, the spring blooms according to the $H$ state terminate earlier than those in the $C$ state, and the Chl concentrations throughout the summer stay lower in the $H$ state in comparison to the $C$ state. It should be noted that the $C$ simulation does not capture the summer Chl peaks occuring at the Norderelbe and Helgoland stations.
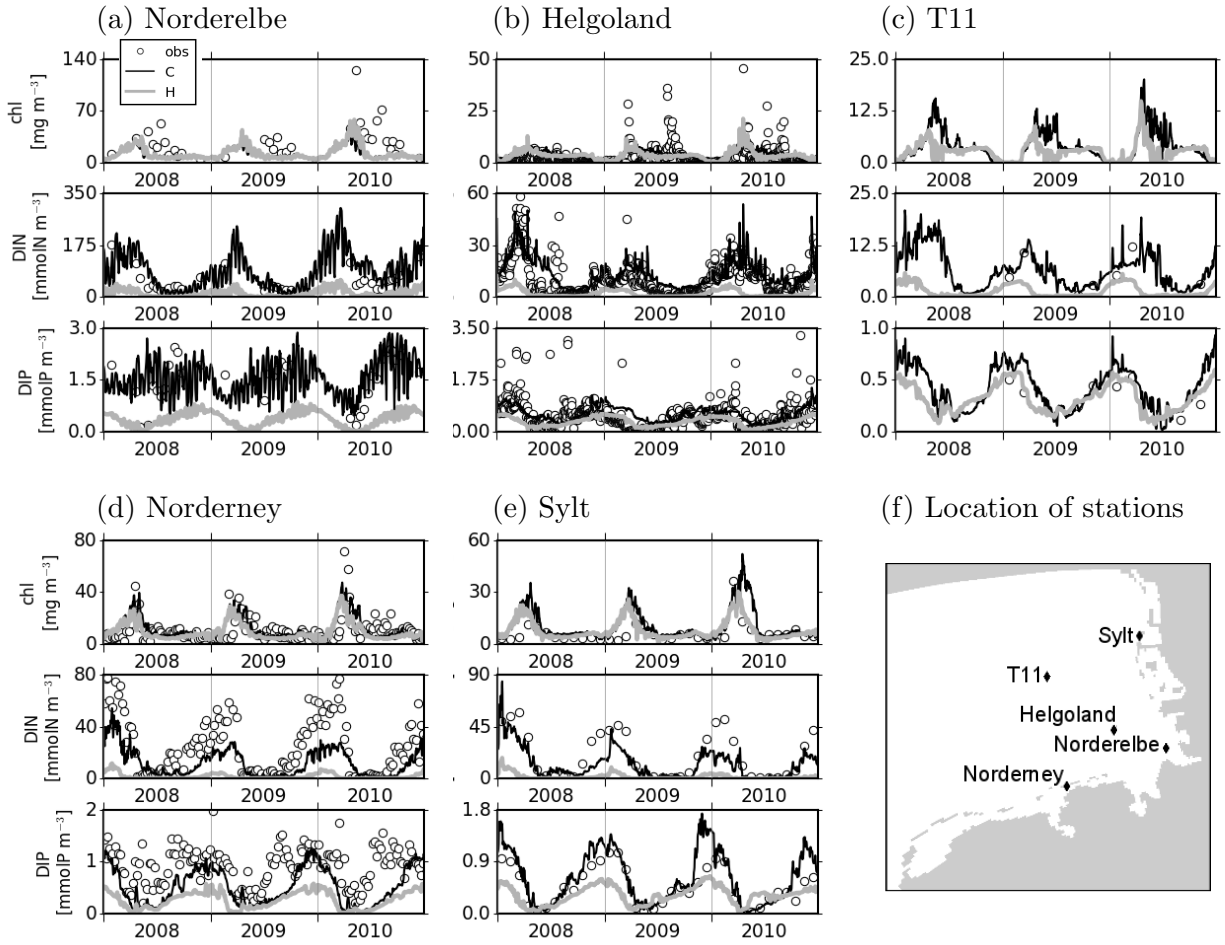
Figure 5: Time series of observed and simulated surface Chl, DIN and DIP concentrations for 3 example years.

*3.3. Elaboration of the differences in phytoplankton under C and H states*

Given the common occurrences of deep Chl maxima in the study system (e.g., Fernand et al., 2013), we consider depth-averaged Chl concentrations to be more informative than the surface values only. Moreover, as the biomass-specific Chl content is subject to variations (e.g., Kruskopf & Flynn, 2006), C bound to phytoplankton (hereafter Phy-C) is worth consideration. In Fig. 6, percentage differences between the *C* and *H* states during the growing season of 2009, based on surface Chl, depth-averaged (D.A.) Chl, and Phy-C are shown.

As the most important departure of the depth-averaged differences in Chl from those at the surface (Fig. 6a,b), the off-shore region with relatively high (>30%) differences disappear and more patches with negligible differences emerge in the latter, implying weaker sensitivity when the entire water column is considered. Differences in depth-averaged Phy-C display entirely dissimilar spatial patterns from the chlorophyll-based metrics, with significant negative differences ($< -10\%$) only within the northern and western margins of the Wadden Sea, and either negligible or significant positive differences (>10%) in large areas (Fig. 6c). The lower Phy-C concentrations within the marginal Wadden Sea are aligned with the gradients in nutrient differences
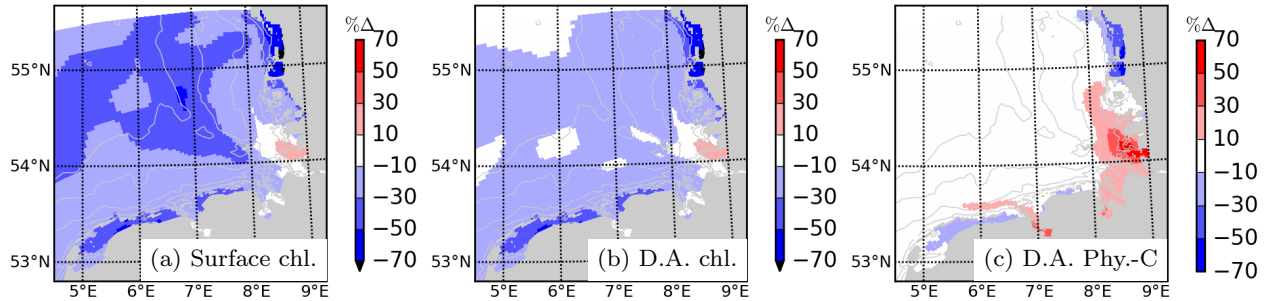
11

Figure 6: 2009 growing season (April–September) average percentage differences obtained under the historic state relative to the control state, for surface Chl (a), depth-averaged (D.A.) Chl (b), and phytoplankton-C (c).

shown in Fig. 4, therefore explained by nutrient limitation. However, the patches of non-significant and even positive differences close to the mouth of Elbe river are not explainable likewise (Fig. 4). In the following, we assess the vertical distribution of Chl in the $C$ and $H$ states, and the relevance of bottom-up (i.e., resource limitation and associated acclimative response) and top-down (i.e., grazing) regulation of phytoplankton in the emergence of these various patterns.

### 3.3.1. Changes in vertical distributions of Chl

Vertical distributions of Chl along the transect mentioned above, where opposing gradients are displayed by the differences in nutrient and Chl concentrations obtained under the $C$ and $H$ states (Figs. 4 and 5) are highlighted in Fig. 7. Within the deeper (>20m) regions, the Chl concentrations at the surface layer are lower under the $H$ state (Fig. 7). In contrast, the concentrations in the deeper layers are either not considerably different during summer, or even higher during spring under the $H$ state (Fig. 7). The insensitivity of the deep-water Chl concentrations explains the lower differences in depth-average values relative to the surface values (Fig. 4). In the inner German Bight, the region within which the Chl concentration is >10mg/m$^3$ during spring extends slightly farther off-shore under the $H$ state. This is consistent with the slightly larger zone of negligible change suggested by the depth-averages relative to the surface values (Fig. 6).

### 3.3.2. Resource limitation

Consistent with the lower nutrient concentrations under the $H$ state (Fig. 4), especially the N but also the P allowances ($A_N$, $A_P$; see Section 2.1.2) of phytoplankton growth are estimated to be much higher under the $H$ state relative to those under the $C$ state (Fig. 8a,b). In contrast, the light allowance of growth ($A_L$) is considerably (up to 30-50%) higher under the $H$ state (Fig. 8c). The higher light allowance under the $H$ state reflects the higher light availability due to the weaker attenuation of light by the lower concentrations of phytoplankton (in some coastal areas), detritus and dissolved inorganic carbon, driven directly by the lower riverine organic matter fluxes (Table 2), and indirectly by lower dissolved inorganic nutrient inputs (Figs. 2-3). The resulting average specific growth rates under the $H$ state suggest mostly off-shore patches of negligible change (Fig. 8d), reflecting the compensation of lower nutrient allowance by the higher light
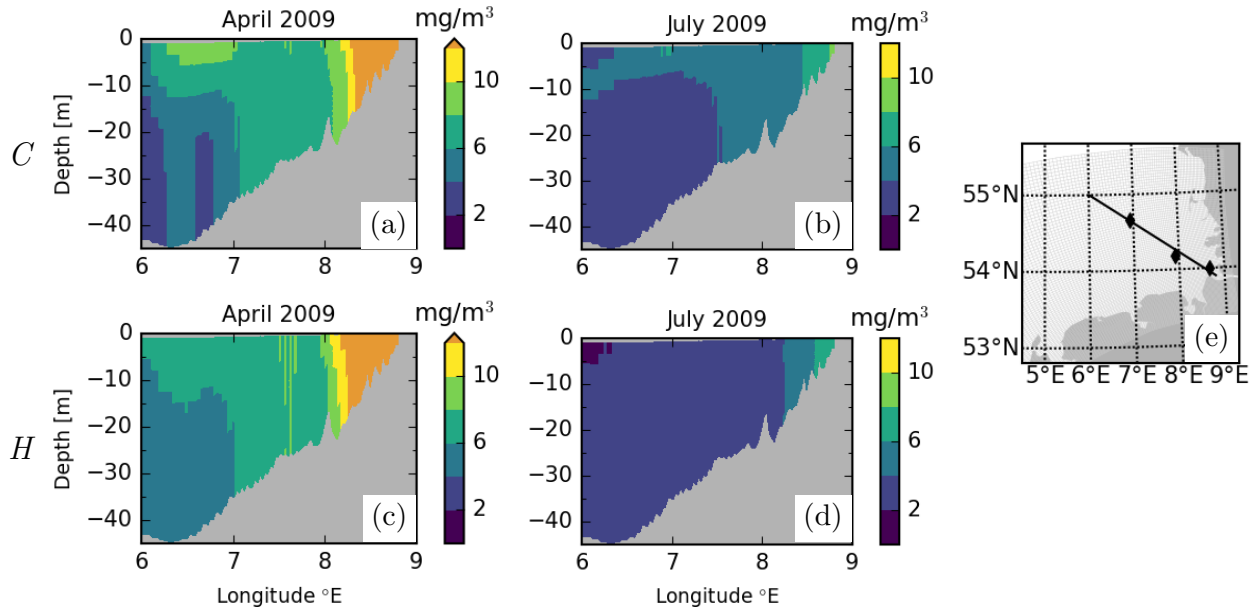
12

Figure 7: Vertical distribution of Chl concentrations averaged over (a,c) April and (b,d) July 2009 estimated for the (a,b) control and (c,d) historic states, along the transect in (e), showing also the stations Norderelbe, Helgoland and T11, analyzed in Fig.5).

allowance. These patches of negligible change in growth rate, in turn, coincide with, hence partially explain the large areas of negligible change in depth-averaged Phy-C (Fig. 6c).
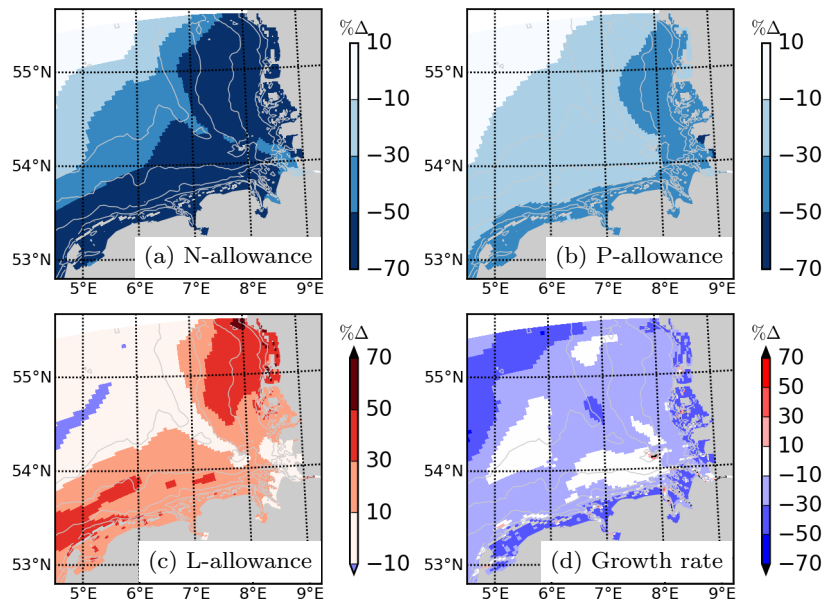


Figure 8: Percentage differences in 2009 growing season (April-September), water column averaged, biomass-weighted N, P and light(L) allowance of growth, and specific growth rate obtained under the historic state relative to the control state.

Differences in light and nutrient availabilities under the $C$ and $H$ states (Fig. 8) affect the estimated

average physiological state of the phytoplankton: Chl:C ratios are higher under the $C$ state than those under the $H$ state (Fig. 9) as well. The lower Chl:C under the $H$ state, in turn, explains the stronger differences in Phy-C relative to Chl concentrations (Fig. 6b,c).
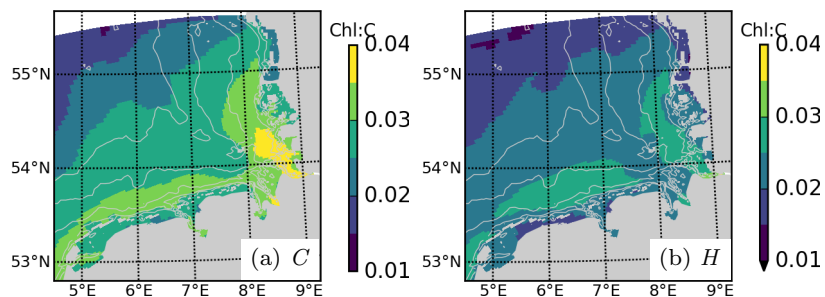


Figure 9: Depth-averaged Chl:C ratio of the phytoplankton during 2009 summer (June-August) estimated for the $C$ and $H$ states.

### 3.3.3. Top-down control

The estimated grazing pressure exerted by the zooplankton under the $H$ state is lower than that in the $C$ state, especially in the coastal regions (up to 50%; Fig. 10a). This explains why Phy-C is not lower in the $H$ state (Fig. 6c) despite the considerably lower growth rates in some regions (Fig. 8). The lower grazing pressure is primarily driven by the lower zooplankton C biomass (Zoo-C, Fig. 10b). The truncation of the Zoo-C under the $H$ state is either stronger than that of Phy-C in the coastal areas, or is in stark contrast with the higher Phy-C within the Elbe plume (Fig. 6c), leading to much higher Phy-C:Zoo-C within the coastal zone under the $H$ state (Fig. 10c). The decoupling of the Zoo-C from the Phy-C is explained by the much lower N and P bound to phytoplankton (hereafter Phy-N and Phy-P, respectively) under the $H$ state (Fig. 10d,e), as the effective assimilation rate of C by the zooplankton depends also on the Phy-N and Phy-P (see Section 2.1.3).

## 4. Discussion

### 4.1. German Bight, and the reconstruction of its historic state

The German Bight was heavily eutrophied until the 1990s, and has been recovering since (Claussen et al., 2009; Wiltshire et al., 2010; van Beusekom et al., 2017). For an evaluation of the ecological status of the system, the reference conditions, representing the minimally perturbed state of the system needs to be known. For the German Bight and the surrounding coastal Wadden Sea, there has been earlier work on the construction of reference states based on statistical methods and budget considerations (van Beusekom, 2005; Brockmann et al., 2007; Topcu et al., 2011). Although these studies have been successful in gaining insight and assisting the management of the system (Claussen et al., 2009), a process-based modelling approach has been lacking so far, which is needed to develop understanding of the specific mechanisms driving the differences between the reference and recent states.
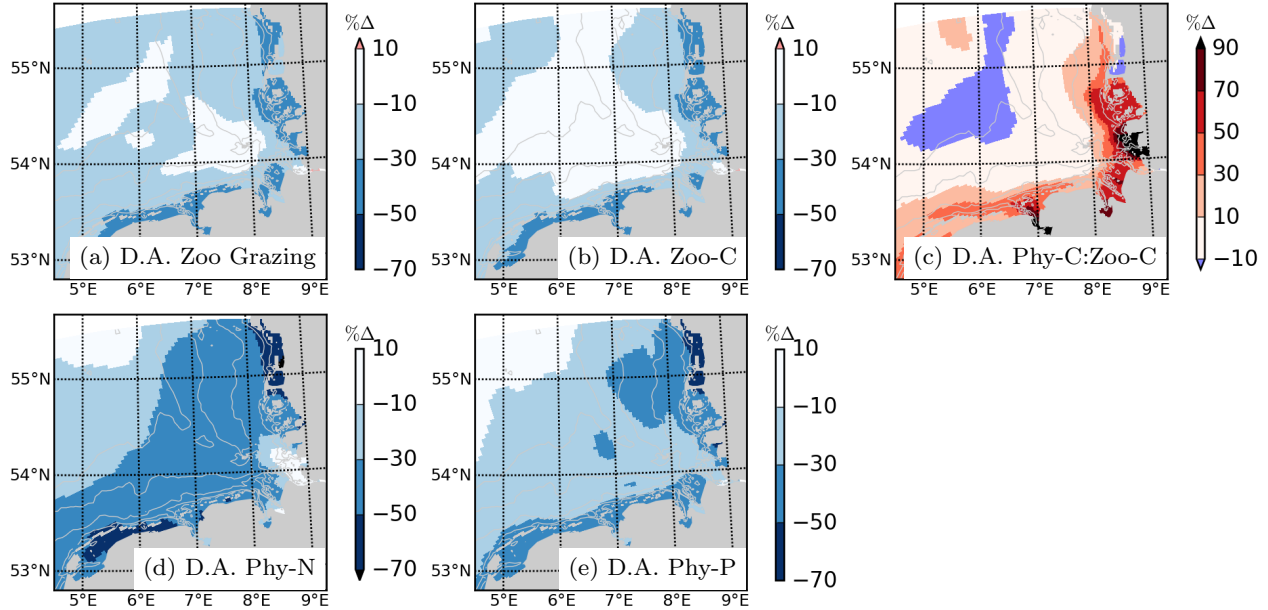
Figure 10: 2009 growing season (April-September) average percentage differences obtained under the historic state relative to the control state, for, depth-average (a) specific grazing rate by zooplankton; (b) C bound to zooplankton; (c) ratio of phytoplankton to zooplankton in terms of C; (d,e): N and P bound to phytoplankton

In the present study, we use such a process-based, coupled physical-biogeochemical modelling framework for constructing the 'historical state' of the German Bight, following similar efforts for the case of the Baltic Sea (Schernewski & Neumann, 2005), southern Bight of the North Sea (Lancelot et al., 2014) and for the North-East Atlantic (Desmit et al., 2015, 2018): we first constructed the nutrient fluxes to the North Sea for the year 1880, which is operationally defined to be the reference state of the system, by combining the present-day discharge rates with the estimated N and P concentrations in major continental rivers by the river basin model MONERIS, and extrapolating the atmospheric deposition estimates back to 1880 (see Section 2.2.2). By keeping all other forcing, i.e., riverine freshwater discharges, meteorological conditions and hydrodynamic conditions at the open boundaries the same as in the control state, we ensured that the resulting differences are only due to the changes in nutrient fluxes.

### 4.2. Mechanisms governing the insensitivity of phytoplankton

Our findings suggest stronger differences in DIN between the historic and recent states than those in DIP. Given the similar levels of reduction factors calculated for the N and P concentrations under the $H$ state (Table 1), this difference is likely due to the much increased atmospheric N deposition rates during the last century 3). The contribution by atmospheric deposition to the N budget is estimated to be about 10-20% in the German Bight (Troost et al., 2013; Große et al., 2017). The difference in growing season surface Chl concentrations is not as pronounced as those in the DIP and DIN concentrations. For the study region, the limited response of surface Chl concentrations to nutrient reductions is in agreement with long-term observations (e.g. Loebl et al., 2009; Vries et al., 1998) and some model estimates (see Lenhart et al., 2010).

15

For the Wadden Sea, relationship between the Chl and winter TN loading is spatially heterogeneous: while there seems to exist a very significant, positive relationship albeit with a high variability of about $\pm 50\%$ within the outer regions, no such significant relationship seems to exist within the inner regions (e.g. van Beusekom et al., 2017). Our findings suggest even lower sensitivity of the depth-averaged phytoplankton carbon biomass than the surface Chl (Fig.6), challenging the reliability of the often used surface Chl as an indicator parameter (e.g., Lenhart et al., 2010; Desmit et al., 2015), especially in deep waters. The insensitivity of phytoplankton concentrations is explained by a combination of two main mechanisms.

First of those mechanisms is the compensation of nutrient limitation by the relaxed light limitation under the $H$ state, mediated by the adaptability of the phytoplankton to these changes in the resource environment. Primary production is strongly limited by light in the inner German Bight and Wadden Sea (e.g. Colijn & Cadée, 2003; Loebl et al., 2009), which is not untypical among coastal/estuarine systems (Cloern, 2001). The simulated light climate is considerably better in the $H$ state (Fig. 8c), due to lower particulate organic matter loads from the rivers. As a result of the improved light climate and the lower pelagic nutrient concentrations in the $H$ state, productivity shifts to the deeper layers of the stratified regions during the summer months (Fig. 7). Below the thermocline, productivity is further supported by the nutrient supply from the sediments (Soetaert & Middelburg, 2009), which is represented in our model system (Kerimoglu et al., 2017). As an adaptive response to the changes in nutrient and light limitation, cellular resource allocations change, as indicated by lower Chl:C under the $H$ state (Fig. 9). According to the model (section 2.1.1, see also Wirtz & Kerimoglu (2016); Kerimoglu et al. (2017)), under the relatively nutrient-scarce, light-replete $H$ state, allocation of cellular resources to the light harvesting machinery is not as beneficial (in terms of growth rate) as in the $C$ state, resulting in lower Chl:C than in the $C$ state. In reality, such an adaptation can be manifested across a wide range of organisational scales, from individual organisms showing plastic responses as observed in monoculture laboratory experiments, to changing irradiance (e.g., Geider et al., 1997) or $CO_2$ concentrations (e.g., Schaum et al., 2012), or to shifts in community structures through species sorting in response to changes in the resource environment (e.g., Philippart et al., 2000; Jochimsen et al., 2012). A similar inter-decadal change in Chl:C has been detected by *in-situ* measurements off the Dutch Coast (Alvarez-Fernandez & Riegman, 2014), which was interpreted as a community-wide response to the changes in nutrient concentrations and light availability in the system. Thus, the acclimative phytoplankton growth model (Wirtz & Kerimoglu, 2016; Kerimoglu et al., 2017) employed in this study realistically accounts for the changes in the average physiological state of the phytoplankton, which would be largely overlooked by a classical model. It should, however, be noted that, although our acclimative model accounts for the changes in resource utilization traits, it entirely ignores other potentially relevant ecological traits, such as the colony formation behavior of *Phaeocystis* and mixotrophic abilities of dinoflagellates (Smayda, 1997), which are frequently observed in the southern North Sea (Lacroix et al., 2007; Loebl et al., 2007; Wollschläger et al., 2015), and were part of the historic phytoplankton (Cadée & Hegeman, 1991; Gieskes et al., 2007).

The second mechanism responsible for the insensitivity of the phytoplankton to lower nutrient loading is

found to be the lower zooplankton biomass, and accordingly, the lower grazing pressure under the $H$ state

340 (Fig. 10). The low zooplankton biomass, in turn, is a result of the low N and P content, i.e., poor nutritional quality of the phytoplankton. Negative effects of the poor food quality (low N:C and/or P:C) on primary consumers have been demonstrated experimentally (e.g., Sterner et al., 1998; Mahlzahn et al., 2010; Hessen et al., 2013; Teurlincx et al., 2017). A number of intriguing consequences of the interaction between the stoichiometrically variable phytoplankton and homeostatic zooplankton have been addressed by previous

345 theoretical work (e.g., Loladze et al., 2000; Grover, 2003; Leroux & Loreau, 2010; Cherif & Loreau, 2013). However, to our knowledge, investigation of the ecosystem-scale relevance of the effects of the nutrient supply rates on the zooplankton nutrition, and in turn, grazing pressure, under a realistic biogeochemical modelling framework has been lacking so far. It should be noted that, although the zooplankton are considered to be stoichiometrically homeostatic at an organismal level, systematic differences are found between different

350 zooplankton groups (Andersen & Hessen, 1991; Gismervik, 1997; Sterner & Elser, 2002), which is not represented by our model. In reality, the decrease in food quality may induce a stoichiometric adjustment of the zooplankton community through shifts in species composition as was observed in the mesocosm experiments of Teurlincx et al. (2017). In fact, shifts in zooplankton community composition have been detected in the North Sea, however, these were associated with changes in hydro-climatic conditions (Alvarez-Fernandez

355 et al., 2012; Beaugrand et al., 2014). Moreover, the unrepresented changes in the ecological traits of the phytoplankton such as their edibility are potentially relevant for the zooplankton community structure as well (e.g., Rousseau et al., 2000). Finally, although the impact of the upper trophic levels on the zooplankton, i.e., the planktivorous fish and the gelatinous zooplankton are mimicked by a quadratic mortality term by our model (Kerimoglu et al., 2017), this approach cannot represent a potential decoupling of the zooplankton

360 biomass and the fish stock in response to the changes in nutrient supply to the system (e.g., Jeppesen et al., 2005; Mahlzahn et al., 2010; Bauer et al., 2018). For a model-based analysis of the changes in the entire food-web structure, an end-to-end modelling framework would be necessary (e.g., Salihoglu et al., 2017). Given these missing components, the reduction in zooplankton biomass under the $H$ state predicted by the model should be considered only as an indication of potential effects on the food-web dynamics in a general

365 sense.

### 4.3. Strengths and limitations of our approach

In this study, we used a modelling framework that was previously shown to have a high skill in the study system, based on comparisons with measurements at fixed monitoring stations, in-situ measurements, satellite imagery and continuous transect data (Kerimoglu et al., 2017). In particular, the model was shown

370 to realistically reproduce the steep coastal gradients in the system (Fig. 4), enabling an assessment of the ecosystem dynamics at the coastal and off-shore areas based on a single model run and parameterization. However, it should be noted that certain features of the system are not reproduced, such as the summer peaks of DIP concentrations observed in some coastal stations (e.g., Fig. 5d), and the summer Chl blooms (e.g., Fig. 5a,b), presumably due to the coarse representation of relevant processes, such as the benthic

17

diagenesis regarding the former and omission of particular phytoplankton groups like the grazing resistant *Phaeocystis*, and zooplankton groups that may have considerably different stoichiometry and feeding behavior (see Kerimoglu et al., 2017). Concerning the aim of the current study to provide insight into the inter-decadal changes in the system, additional limitations need to be taken into consideration. For instance, the projected improvement in the light climate driven by the reduction of particulate organic matter is subject to uncertainties, given the partial information on the stoichiometry of the riverine loads and partitioning of the organic matter into the particulate and dissolved forms, and potential differences in these coefficients in the historic and recent states of the system (Brockmann, 1994; Amann et al., 2012). Manipulation of the estuaries during the past century possibly diminished their denitrification potential (de Jonge & de Jong, 2002; Dähnke et al., 2008; Deek et al., 2013). We attempted to account for this by assuming the historic riverine TN loads to be 50% lower than those estimated by the MONERIS model, which represents the upper bound of estuarine nitrogen removal estuaries (Seitzinger, 1988). However, this assumption is subject to large uncertainties and needs refinement in future studies. Moreover, the static forcing field we used to describe the light attenuation caused by the suspended particulate matter cannot capture the potential inter-decadal changes in the system (e.g., de Jonge & de Jong, 2002). Finally, the seagrass, which had a wider coverage within the historic Wadden Sea (Reise & Kohlus, 2008), in reality, could have, suppressed the phytoplankton concentrations in the coastal regions, by acting as a sink term for the nutrients, and reducing the benthic nutrient effluxes by stabilizing the sediments (McGlathery et al., 2007). The limited understanding of these individual factors, and their interactions points to the need for continued efforts for a better representation of long-term changes in the system. Given these shortcomings, specific predictions of our model, such as the nutrient and phytoplankton concentrations in the historic state might be inaccurate. Nevertheless, accounting for the adaptability of the phytoplankton to the changes in their resource environment, and associated variations in their Chl:C:N:P in our modelling framework allowed the assessment of the role of these flexibilities in shaping their response to the changes in nutrient inputs and led to novel insights; foremost the adaptive capacity of phytoplankton to buffer environmental change as indicated by lower Chl:C, and disproportional decreases in zooplankton biomass due to poor nutritional quality (lower N:C and P:C) under the pristine state. Thereby, our study highlights the potential relevance of the adaptation processes when assessing long-term changes.

## 5. Conclusions

Using a 3-D coupled physical-biogeochemical modelling framework, and realistic estimations of nutrient fluxes, the historic (1880s) state of the German Bight biogeochemistry was consistently reconstructed and compared with the recent (2000-2010) state. The surface DIN and DIP concentrations in the historic state differ from those in the recent state most strongly (>50%) along the coastal stripe of the German Bight. Differences in surface Chl concentrations are in general much weaker and display complex patterns. Differences between the two states are even weaker, when the depth-averaged phytoplankton biomass is considered. The lack of reduction in phytoplankton biomass under the $H$ state is explained by; 1) the better light climate due

to lower organic material loadings by rivers and acclimative capacity of the phytoplankton; 2) lower grazing pressure by lower zooplankton biomass, caused by the poor food quality (low N:C and P:C in phytoplankton). Representation of both of these processes were allowed by the flexible Chl:C:N:P of the phytoplankton resolved by the optimality based, acclimative model of phytoplankton growth. This is significant, and calls attention, given that the adaptation processes and physiological plasticity are usually ignored in model-based sensitivity analyses, not only concerning the impacts of eutrophication, but also other stressors, such as climate warming and acidification.

**References**

Alvarez-Fernandez, S., Lindeboom, H., & Meesters, E. (2012). Temporal changes in plankton of the North Sea: Community shifts and environmental drivers. *Marine Ecology Progress Series*, *462*, 21–38. doi:`10.3354/meps09817`.

Alvarez-Fernandez, S., & Riegman, R. (2014). Chlorophyll in North Sea coastal and offshore waters does not reflect long term trends of phytoplankton biomass. *Journal of Sea Research*, *91*, 35–44. doi:`10.1016/j.seares.2014.04.005`.

Amann, T., Weiss, A., & Hartmann, J. (2012). Carbon dynamics in the freshwater part of the Elbe estuary, Germany: Implications of improving water quality. *Estuarine, Coastal and Shelf Science*, *107*, 112–121. doi:`10.1016/j.ecss.2012.05.012`.

Andersen, T., & Hessen, D. O. (1991). Carbon, nitrogen, and phosphorus content of freshwater zooplankton. *Limonology And Oceanography*, *36*, 807–814.

Artioli, Y., Friedrich, J., Gilbert, A. J., McQuatters-Gollop, A., Mee, L. D., Vermaat, J. E., Wulff, F., Humborg, C., Palmeri, L., & Pollehne, F. (2008). Nutrient budgets for European seas: a measure of the effectiveness of nutrient reduction policies. *Marine pollution bulletin*, *56*, 1609–17. doi:`10.1016/j.marpolbul.2008.05.027`.

Bauer, B., Meier, H. E. M., Casini, M., Hoff, A., Orio, A., Saraiva, S., Steenbeek, J., & Tomczak, M. T. (2018). Reducing eutrophication increases spatial extent of communities supporting commercial fisheries: a model case study. *ICES Journal of Marine Science*, . doi:`10.1093/icesjms/fsy003`.

Beaugrand, G., Harlay, X., & Edwards, M. (2014). Detecting plankton shifts in the North Sea: A new abrupt ecosystem shift between 1996 and 2003. *Marine Ecology Progress Series*, *502*, 85–104. doi:`10.3354/meps10693`.

van Bennekom, A., & Wetsteijn, F. (1990). The winter distribution of nutrients in the southern bight of the north sea (1961-1978) and in the estuaries of the scheldt and the rhine/meuse. *Netherlands Journal of Sea Research*, *25*, 75–87.

van Beusekom, J. E., Bot, P., Carstensen, J., Grage, A., Kolbe, K., Lenhart, H.-J., Pätsch, J., Petenati, T., & Rick, J. (2017). Eutrophication. In S. Kloepper (Ed.), *Wadden Sea Quality Status Report 2017.*. Wilhelmshaven, Germany: Common Wadden Sea Secretariat.

van Beusekom, J. E., & de Jonge, V. N. (2002). Long-term changes in Wadden Sea nutrient cycles: importance of organic matter import from the North Sea. *Hydrobiologia*, *475/476*, 185–194. doi:`10.1023/A:1020361124656`.

van Beusekom, J. E. E. (2005). A historic perspective on Wadden Sea eutrophication. *Helgoland Marine Research*, *59*, 45–54. doi:`10.1007/s10152-004-0206-2`.

Bricker, S. B., Ferreira, J. G., & Simas, T. (2003). An integrated methodology for assessment of estuarine trophic status. *Ecological Modelling*, *169*, 39–60. doi:`10.1016/S0304-3800(03)00199-6`.

Brockmann, U., Topcu, D., & Schütt, M. (2007). *Assessment of the eutrophication status of the German Bight according to the OSPAR Comprehensive Procedure*. Technical Report Hamburg.

Brockmann, U. H. (1994). Organic matter in the Elbe estuary. *Netherlands Journal of Aquatic Ecology*, *28*, 371–381. doi:`10.1007/BF02334207`.

Bruggeman, J., & Bolding, K. (2014). A general framework for aquatic biogeochemical models. *Environmental Modelling & Software*, *61*, 249–265. doi:`10.1016/j.envsoft.2014.04.002`.

Burchard, H., & Bolding, K. (2002). *GETM: A general estuarine transport model*. Technical Report Joint Research Centre Ispra, Italy.

Burchard, H., Flöser, G., Staneva, J. V., Badewien, T. H., & Riethmüller, R. (2008). Impact of Density Gradients on Net Sediment Transport into the Wadden Sea. *Journal of Physical Oceanography*, *38*, 566–587. doi:`10.1175/2007JPO3796.1`.

Cadée, G. C., & Hegeman, J. (1991). Historical phytoplankton data of the marsdiep. *Hydrobiological Bulletin*, *24*, 111–118.

Cai, W.-j., Hu, X., Huang, W.-j., Murrell, M. C., Lehrter, J. C., Lohrenz, S. E., Chou, W.-c., Zhai, W., Hollibaugh, J. T., Wang, Y., Zhao, P., Guo, X., Gundersen, K., Dai, M., & Gong, G.-c. (2011). Acidification of subsurface coastal waters enhanced by eutrophication. *Nature Geoscience*, *4*, 766–770. doi:`10.1038/ngeo1297`.

Callies, U., & Scharfe, M. (2015). Mean spring conditions at Helgoland Roads, North Sea: Graphical modeling of the influence of hydro-climatic forcing and Elbe River discharge. *Journal of Sea Research*, *101*, 1–11. doi:`10.1016/j.seares.2014.06.008`.

Cherif, M., & Loreau, M. (2013). Plant herbivore decomposer stoichiometric mismatches and nutrient cycling in ecosystems. *Proceedings of the Royal Society B*, *280*, 20122453.

CIS-COAST (2003). *Transitional and Coastal Waters Typology, Reference Conditions and Classification Systems, Common Implementation Strategy for the Water Framework Directive (2000/60/EC), Guidance document no.5*. Technical Report European Communities.

Claussen, U., Zevenboom, W., Brockmann, U., Topcu, D., & Bot, P. (2009). Assessment of the eutrophication status of transitional, coastal and marine waters within OSPAR. *Hydrobiologia*, *629*, 49–58. doi:`10.1007/s10750-009-9763-3`.

Cloern, J. E. (2001). Our evolving conceptual model of the coastal eutrophication problem. *Marine Ecology Progress Series*, *210*, 223–253.

Colijn, F., & Cadée, G. C. (2003). Is phytoplankton growth in the Wadden Sea light or nitrogen limited ? *Journal of Sea Research*, *49*, 83 – 93. doi:`10.1016/S1385-1101(03)00002-9`.

Dähnke, K., Bahlmann, E., & Emeis, K. (2008). A nitrate sink in estuaries? An assessment by means of stable nitrate isotopes in the Elbe estuary. *Limnology and Oceanography*, *53*, 1504–1511. doi:`10.4319/lo.2008.53.4.1504`.

Deek, A., Dähnke, K., Van Beusekom, J., Meyer, S., Voss, M., & Emeis, K. (2013). N2 fluxes in sediments of the Elbe Estuary and adjacent coastal zones. *Marine Ecology Progress Series*, *493*, 9–21. doi:`10.3354/meps10514`.

Desmit, X., Lacroix, G., Dulière, V., Lancelot, C., Gypens, N., Ménesguen, A., Thouvenin, B., Dussauze, M., Billen, G., Garnier, J., Thieu, V., Silvestre, M., Passy, P., Lasaletta, L., Guittard, G., Théry, S., Neves, R., Campuzano, F., Garcia, C., Pinto, L., Sobrinho, J., Mateus, M., & Ascione Kenov, I. (2015). *Ecosystem Models as Support to Eutrophication Management in the North Atlantic Ocean (EMoSEM). EMoSEM Final Report EU FP7 Seas-Era Project*. Technical Report Royal Belgian Institute for Natural Sciences (RBINS).

Desmit, X., Thieu, V., Billen, G., Campuzano, F., Dulière, V., Garnier, J., Lassaletta, L., Ménesguen, A., Neves, R., Pinto, L., Silvestre, M., Sobrinho, J. L., & Lacroix, G. (2018). Reducing marine eutrophication may require a paradigmatic change. *Science of the Total Environment*, *635*, 1444–1466. doi:`10.1016/j.scitotenv.2018.04.181`.

Diaz, R. J., & Rosenberg, R. (2008). REVIEW Spreading Dead Zones and Consequences for Marine Ecosystems. *Science*, *321*, 926–930.

Duarte, C. M., Conley, D. J., Carstensen, J., & Sánchez-Camacho, M. (2009). Return to Neverland : Shifting Baselines Affect Eutrophication Restoration Targets. *Estuaries and Coasts*, *32*, 29–36. doi:`10.1007/s12237-008-9111-2`.

EC (2000). Directive 2000/60/EC of the European Parliament and of the Council of 23 October 2000 establishing a framework for Community action in the field of water policy. *Official Journal of the European Parliament*, *L327*, 1–82. doi:`10.1039/ap9842100196`.

EC (2009). *Common implementation strategy for the water framework directive (2000/60/EC). Guidance Document No. 23*. Technical Report.

Emeis, K. C., van Beusekom, J., Callies, U., Ebinghaus, R., Kannen, A., Kraus, G., Kröncke, I., Lenhart, H., Lorkowski, I., Matthias, V., Möllmann, C., Pätsch, J., Scharfe, M., Thomas, H., Weisse, R., & Zorita, E. (2015). The North Sea - A shelf sea in the Anthropocene. *Journal of Marine Systems*, *141*, 18–33. doi:`10.1016/j.jmarsys.2014.03.012`.

Fernand, L., Weston, K., Morris, T., Greenwood, N., Brown, J., & Jickells, T. (2013). The contribution of the deep chlorophyll maximum to primary production in a seasonally stratified shelf sea, the North Sea. *Biogeochemistry*, *113*, 153–166. doi:`10.1007/s10533-013-9831-7`.

Flöser, G., Burchard, H., & Riethmüller, R. (2011). Observational evidence for estuarine circulation in the German Wadden Sea. *Continental Shelf Research*, *31*, 1633–1639. doi:http://dx.doi.org/10.1016/j.csr.2011.03.014.

Gadegast, M., & Venohr, M. (2015). *Modellierung historischer Nährstoffeinträge und -frachten zur Ableitung von Nährstoffreferenz- und Orientierungswerten für mitteleuropäische Flussgebiete*. Technical Report Leibniz-Institut für Gewässerökologie und Binnenfischerei im Forschungsverbund Berlin e.V. Berlin.

Geider, R., MacIntyre, H., & Kana, T. (1997). Dynamic model of phytoplankton growth and acclimation: responses of the balanced growth rate and the chlorophyll a:carbon ratio to light, nutrient-limitation and temperature. *Marine Ecology Progress Series*, *148*, 187–200.

Gieskes, W., Leterme, S., Peletier, H., Edwards, M., & Reid, P. (2007). colony distribution in the North Atlantic Ocean since 1948, and interpretation of long-term changes in the. *Biogeochemistry*, *83*, 49–60. doi:10.1007/s10533-007-9082-6.

Gismervik, I. (1997). Stoichiometry of some marine planktonic crustaceans. *Journal of Plankton Research*, *19*, 279–285.

Große, F., Greenwood, N., Kreus, M., Lenhart, H. J., Machoczek, D., Pätsch, J., Salt, L. A., & Thomas, H. (2016). Looking beyond stratification: a model-based analysis of the biological drivers of oxygen deficiency in the North Sea. *Biogeosciences*, *13*, 2511–2535. doi:10.5194/bgd-12-12543-2015.

Große, F., Kreus, M., Lenhart, H.-J., Pätsch, J., & Pohlmann, T. (2017). A Novel Modeling Approach to Quantify the Influence of Nitrogen Inputs on the Oxygen Dynamics of the North Sea. *Frontiers in Marine Science*, *4*, 1–21. doi:10.3389/fmars.2017.00383.

Grover, J. (2003). The Impact of Variable Stoichiometry on PredatorPrey Interactions: A Multinutrient Approach. *The American Naturalist*, *162*, 29–43.

Hessen, D. O., Elser, J. J., Sterner, R. W., & Urabe, J. (2013). Ecological stoichiometry: An elementary approach using basic principles. *Limnology and Oceanography*, *58*, 2219–2236. doi:10.4319/lo.2013.58.6.2219.

Hirt, U., Mahnkopf, J., Gadegast, M., Czudowski, L., Mischke, U., Heidecke, C., Schernewski, G., & Venohr, M. (2014). Reference conditions for rivers of the German Baltic Sea catchment: reconstructing nutrient regimes using the model MONERIS. *Regional Environmental Change*, *14*, 1123–1138. doi:10.1007/s10113-013-0559-7.

Jeppesen, E., Jensen, J. P., Søndergaard, M., & Lauridsen, T. L. (2005). Response of fish and plankton to nutrient loading reduction in eight shallow Danish lakes with special emphasis on seasonal dynamics. *Freshwater Biology*, *50*, 1616–1627. doi:10.1111/j.1365-2427.2005.01413.x.

Jochimsen, M. C., Kummerlin, R., & Straile, D. (2012). Compensatory dynamics and the stability of phytoplankton biomass during four decades of eutrophication and oligotrophication. *Ecology Letters*, *16*, 81–89. doi:`10.1111/ele.12018`.

de Jonge, V. N., & de Jong, D. J. (2002). 'Global Change' Impact of Inter-Annual Variation in Water Discharge as a Driving Factor to Dredging and Spoil Disposal in the River Rhine System and of Turbidity in the Wadden Sea. *Estuarine, Coastal and Shelf Science*, *55*, 969–991. doi:`10.1006/ecss.2002.1039`.

Jülich Supercomputing Centre (2016). JURECA: General-purpose supercomputer at Jülich Supercomputing Centre. *Journal of large-scale research facilities*, *2*. doi:`10.17815/jlsrf-2-121`.

Kerimoglu, O., Hofmeister, R., Maerz, J., Riethmüller, R., & Wirtz, K. W. (2017). The acclimative biogeochemical model of the southern North Sea. *Biogeosciences*, *14*, 4499–4531. doi:`10.5194/bg-14-4499-2017`.

Kruskopf, M., & Flynn, K. J. (2006). Chlorophyll content and fluorescence responses cannot be used to gauge reliably phytoplankton biomass, nutrient status or growth rate. *New Phytologist*, *169*, 525–536. doi:`10.1111/j.1469-8137.2005.01601.x`.

Laane, R. W. P. M., Brockmann, U., Van Liere, L., & Bovelander, R. (2005). Immission targets for nutrients (N and P) in catchments and coastal zones: A North Sea assessment. *Estuarine, Coastal and Shelf Science*, *62*, 495–505. doi:`10.1016/j.ecss.2004.09.013`.

Lacroix, G., Ruddick, K., Gypens, N., & Lancelot, C. (2007). Modelling the relative impact of rivers (Scheldt/Rhine/Seine) and Western Channel waters on the nutrient and diatoms/ Phaeocystis distributions in Belgian waters (Southern North Sea). *Continental Shelf Research*, *27*, 1422–1446. doi:`10.1016/j.csr.2007.01.013`.

Lancelot, C., Passy, P., & Gypens, N. (2014). Model assessment of present-day Phaeocystis colony blooms in the Southern Bight of the North Sea (SBNS) by comparison with a reconstructed pristine situation. *Harmful Algae*, *37*, 172–182. doi:`10.1016/j.hal.2014.05.017`.

Laurent, A., Fennel, K., Hu, J., & Hetland, R. (2012). Simulating the effects of phosphorus limitation in the Mississippi and Atchafalaya river plumes. *Biogeosciences*, *9*, 4707–4723. doi:`10.5194/bg-9-4707-2012`.

Lenhart, H.-J., Mills, D. K., Baretta-Bekker, H., van Leeuwen, S. M., van der Molen, J., Baretta, J. W., Blaas, M., Desmit, X., Kühn, W., Lacroix, G., Los, H. J., Ménesguen, A., Neves, R., Proctor, R., Ruardij, P., Skogen, M. D., Vanhoutte-Brunier, A., Villars, M. T., & Wakelin, S. L. (2010). Predicting the consequences of nutrient reduction on the eutrophication status of the North Sea. *Journal of Marine Systems*, *81*, 148–170. doi:`10.1016/j.jmarsys.2009.12.014`.

Leroux, S., & Loreau, M. (2010). Consumer-mediated recycling and cascading trophic interactions. *Ecology*, *91*, 2162–2171.

Loebl, M., Colijn, F., van Beusekom, J., Baretta-Bekker, J., Lancelot, C., Philippart, C., Rousseau, V., & Wiltshire, K. (2009). Recent patterns in potential phytoplankton limitation along the Northwest European continental coast. *Journal of Sea Research*, *61*, 34–43. doi:10.1016/j.seares.2008.10.002.

Loebl, M., Dolch, T., & Beusekom, J. E. E. V. (2007). Annual dynamics of pelagic primary production and respiration in a shallow coastal basin. *Journal of Sea Research*, *58*, 269 – 282. doi:10.1016/j.seares.2007.06.003.

Loladze, I., Kuang, Y., & Elser, J. J. (2000). Stoichiometry in ProducerGrazer Systems: Linking Energy Flow with Element Cycling. *Bulletin of Mathematical Biology*, *62*, 1137–1162. doi:10.1006/bulm.2000.0201.

Lorkowski, I., Pätsch, J., Moll, A., & Kühn, W. (2012). Interannual variability of carbon fluxes in the North Sea from 1970 to 2006 - Competing effects of abiotic and biotic drivers on the gas-exchange of CO 2. *Estuarine, Coastal and Shelf Science*, *100*, 38–57. doi:10.1016/j.ecss.2011.11.037.

Macias, D., & Stips, A. (2017). Major fertilization sources and mechanisms for Mediterranean Sea coastal ecosystems. *Limnology and Oceanography*, . doi:10.1002/lno.10677.

Mahlzahn, A. M., Hantzsche, F., Schoo, K. L., Boersma, M., & Aberle, N. (2010). Differential effects of nutrient-limited primary production on primary, secondary or tertiary consumers. *Oecologia*, *162*, 35–48. doi:10.1007/s00442-009-1458-y.

McGlathery, K. J., Sundbäck, K., & Anderson, I. C. (2007). Eutrophication in shallow coastal bays and lagoons: the role of plants in the coastal filter. *Marine Ecology Progress Series*, *348*, 1–18. doi:10.3354/meps07132.

Neumann, T., Fennel, W., & Kremp, C. (2002). Experimental simulations with an ecosystem model of the Baltic Sea: A nutrient load reduction experiment. *Global Biogeochemical Cycles*, *16*, 1033. doi:10.1029/2001GB001450.

Nielsen, S. L., Sand-Jensen, K., Borum, J., & Geertz-Hansen, O. (2002). Phytoplankton, Nutrients, and Transparency in Danish Coastal Waters. *Estuaries*, *25*, 930–937.

OSPAR (2013). *Common Procedure for the Identification of the Eutrophication Status of the OSPAR Maritime Area (Reference number: 2013-8)*. Technical Report.

Pätsch, J., Lenhart, H.-J., & Schütt, M. (2016). *Daily Loads of Nutrients, Total Alkalinity, Dissolved Inorganic Carbon and Dissolved Organic Carbon of the European Continental Rivers for the Years 1977–2014*. Technical Report Institut für Meereskunde, Universität Hamburg Hamburg. URL: https://wiki.cen.uni-hamburg.de/ifm/ECOHAM/DATA{_}RIVER?action=AttachFile{&}do=view{&}target=RIVER{_}feb{_}2016.pdf.

Pätsch, J., Serna, A., Dähnke, K., Schlarbaum, T., Johannsen, A., & Emeis, K.-C. (2010). Nitrogen cycling in the German Bight (SE North Sea) Clues from modelling stable nitrogen isotopes. *Continental Shelf Research*, *30*, 203–213. doi:`10.1016/j.csr.2009.11.003`.

Philippart, C., Cadee, G., van Raaphorst, W., & Riegman, R. (2000). Long-term phytoplanktonnutrient interactions in a shallow coastal sea: Algal community structure, nutrient budgets, and denitrification potential. *Limnology and Oceanography*, *45*, 131–144.

van Raaphorst, W., de Jonge, V. N., Dijkhuizen, D., & Frederiks, B. (2000). *Natural background concentrations of phosphorus and nitrogen in the Dutch Wadden Sea*. Technical Report RIKZ The Hague.

Radach, G., & Pätsch, J. (2007). Variability of Continental Riverine Freshwater and Nutrient Inputs into the North Sea for the Years 1977 2000 and Its Consequences for the Assessment of Eutrophication. *Estuaries and Coasts*, *30*, 66–81. doi:`10.1007/BF02782968`.

Reise, K., & Kohlus, J. (2008). Seagrass recovery in the Northern Wadden Sea? *Helgoland*, *62*, 77–84. doi:`10.1007/s10152-007-0088-1`.

Rousseau, V., Becquevort, S., Gasparini, S., Tackx, M., & Lancelot, C. (2000). Trophic efficiency of the planktonic food web in a coastal ecosystem dominated by Phaeocystis colonies. *Journal of Sea Research*, *43*, 357–372.

Salihoglu, B., Arkin, S. S., Akoglu, E., & Fach, B. A. (2017). Evolution of Future Black Sea Fish Stocks under Changing Environmental and Climatic Conditions. *Frontiers in Marine Science*, *4*, 339. doi:`10.3389/fmars.2017.00339`.

Schaum, E., Rost, B., Millar, A. J., & Collins, S. (2012). Variation in plastic responses of a globally distributed picoplankton species to ocean acidification. *Nature Climate Change*, *3*, 298–302. doi:`10.1038/nclimate1774`.

Schernewski, G., & Neumann, T. (2005). The trophic state of the Baltic Sea a century ago: a model simulation study. *Journal of Marine Systems*, *53*, 109–124. doi:`10.1016/j.jmarsys.2004.03.007`.

Schöpp, W., Posch, M., Mylona, S., Johansson, M., Posch, M., Mylona, S., & Johansson, M. (2003). Long-term development of acid deposition (1880-2030) in sensitive freshwater regions in Europe. *Hydrology and Earth System Sciences*, *7*, 436–446.

Schröder, F., Wiltshire, K., Klages, D., Mathieu, B., & Knauth, H.-D. (1996). Nitrogen and oxygen processes in sediments of the Elbe estuary. *Arch. Hydrobiol./Suppl.*, *110*, 311–328.

Seitzinger, S. P. (1988). Denitrification in freshwater and coastal marine ecosystems: Ecological and geochemical significance. *Limnology and Oceanography*, *33*, 702–724. doi:`10.4319/lo.1988.33.4_part_2.0702`.

Smayda, T. J. (1997). Harmful algal blooms: Their ecophysiology and general relevance to phytoplankton blooms in the sea. *Limnology and Oceanography*, *42*, 1137–1153.

Smith, V. H. (2006). Responses of estuarine and coastal marine phytoplankton to nitrogen and phosphorus enrichment. *Limnology and Oceanography*, *51*, 377–384.

Smith, V. H., & Schindler, D. W. (2009). Eutrophication science: where do we go from here? *Trends in Ecology & Evolution*, *24*, 201–207. doi:`10.1016/j.tree.2008.11.009`.

Soetaert, K., & Middelburg, J. J. (2009). Modeling eutrophication and oligotrophication of shallow-water marine systems: the importance of sediments under stratified and well-mixed conditions. *Hydrobiologia*, *629*, 239–254. doi:`10.1007/s10750-009-9777-x`.

Sterner, R., Clasen, J., Lampert, W., & Weisse, T. (1998). Carbon:phosphorus stoichiometry and food chain production. *Ecology Letters*, *1*, 146–150.

Sterner, R., & Elser, J. (2002). *Ecological Stoichiometry: The Biology of Elements from Molecules to the Biosphere*.

Teurlincx, S., Velthuis, M., Seroka, D., Govaert, L., van Donk, E., Van de Waal, D. B., & Declerck, S. A. J. (2017). Species sorting and stoichiometric plasticity control community C:P ratio of first-order aquatic consumers. *Ecology Letters*, *20*, 751–760. doi:`10.1111/ele.12773`.

Topcu, D., Behrendt, H., Brockmann, U., & Claussen, U. (2011). Natural background concentrations of nutrients in the German Bight area (North Sea). *Environmental monitoring and assessment*, *174*, 361–88. doi:`10.1007/s10661-010-1463-y`.

Troost, T. A., Blaas, M., & Los, F. J. (2013). The role of atmospheric deposition in the eutrophication of the North Sea: a model analysis. *J. Marine Syst.*, *125*, 101–112. doi:`10.1016/j.jmarsys.2012.10.005`.

Venohr, M., Hirt, U., Hofmann, J., Opitz, D., Gericke, A., Wetzig, A., Natho, S., Neumann, F., Hürdler, J., Matranga, M., Mahnkopf, J., Gadegast, M., & Behrendt, H. (2011). Modelling of Nutrient Emissions in River Systems MONERIS Methods and Background. *International Review of Hydrobiology*, *96*, 435–483. doi:`10.1002/iroh.201111331`.

Vries, I. D., Duin, R. N. M., Peeters, J. C. H., Los, F. J., Bokhorst, M., & Laane, R. W. P. M. (1998). Patterns and trends in nutrients and phytoplankton in Dutch coastal waters: comparison of time-series analysis, ecological model simulation, and mesocosm experiments. *ICES Journal of Marine Science*, *55*, 620–634.

Wiltshire, K. H., Kraberg, A., Bartsch, I., Boersma, M., Franke, H.-D., Freund, J., Gebühr, C., Gerdts, G., Stockmann, K., & Wichels, A. (2010). Helgoland Roads, North Sea: 45 Years of Change. *Estuaries and Coasts*, *33*, 295–310. doi:`10.1007/s12237-009-9228-y`.

Wirtz, K., & Kerimoglu, O. (2016). Optimality and variable co-limitation controls autotrophic stoichiometry. *Frontiers in Ecology and Evolution*, *4*, 131. doi:10.3389/fevo.2016.00131.

Wollschläger, J., Wiltshire, K. H., Petersen, W., & Metfies, K. (2015). Analysis of phytoplankton distribution and community structure in the German Bight with respect to the different size classes. *Journal of Sea Research*, *99*, 83–96. doi:10.1016/j.seares.2015.02.005.

700